

MECHANICAL PROPERTIES OF FIBER REINFORCED PORE FREE CONCRETE WITH HIGH STRENGTH MATRIX ABOVE 400 MPa

Ryohei Yanagida (1), Takuro Nakamura (1), Katsuya Kono (2) and Junichiro Niwa (1)

(1) Tokyo Institute of Technology, Tokyo, Japan

(2) Taiheiyo cement corporation, Chiba, Japan

Abstract

A new cementitious composite with the extremely high compressive strength has been developed in Japan and named as Pore Free Concrete (PFC). To achieve the maximum density in the binder composition of the PFC, the multiple types of particles are packed as closely as possible based on the closest packing theory proposed by Furnas. The curing process for PFC is divided into three parts; the deaerating process, the steam curing process and the heat curing process under 200 °C. These procedures enable PFC to have a pore-free matrix and the high compressive strength above 400 MPa. However, the mechanical properties of PFC and the influence of the fibers on each mechanical property have not been clarified yet. This study aims to investigate the mechanical properties of PFC reinforced with steel fibers, such as the compressive strength, fracture energy and tension softening curve from experiments. In addition, the finite element analysis using mechanical properties of fiber-reinforced PFC were carried out to investigate the size dependence of flexural strength.

Résumé

Un nouveau composite cimentaire avec une très haute résistance à la compression a été développé au Japon et appelé Pore Free Concrete (PFC). Pour atteindre une densité maximale dans la composition du liant du PFC, de nombreux types de particules ont été empilés le plus étroitement possible selon la théorie de l'empilement maximum proposée par Furnas. Le processus de traitement pour le PFC est divisé en trois étapes : le procédé de désaération, la cure en vapeur et un traitement thermique en dessous de 200°C. Ces procédés permettent au PFC d'avoir une matrice sans pores et une haute résistance en compression, supérieure à 400 MPa. Cependant, les propriétés mécaniques du PFC et l'influence des fibres sur chaque propriété mécanique n'ont pas encore été élucidées. L'objectif de cette étude est d'étudier expérimentalement les propriétés mécaniques du PFC renforcé par des fibres d'acier, comme la résistance en compression, l'énergie de rupture et la réponse adoucissante en traction. De plus des analyses aux éléments finis utilisant les propriétés mécaniques du PFC armé de fibres ont été effectuées pour étudier les effets d'échelle sur sa résistance en flexion.

1. INTRODUCTION

A new cementitious composite with the extremely high compressive strength has been developed in Japan and named as Pore Free Concrete (PFC) [1]. To achieve the maximum density in the binder composition of the PFC, the multiple types of particles are packed as closely as possible based on the closest packing theory proposed by Furnas [2]. The curing process is divided into three parts; the deaerating and water absorbing process, the steam curing process and the heat curing process under 200 °C. These procedures enable PFC to have a pore-free matrix and the high compressive strength of more than 400 MPa.

The purpose of this study is to investigate the mechanical properties of PFC reinforced with short steel fibers. The experimental program includes three issues; to investigate the compression properties by the compression test, the tensile properties by the splitting cylinder test and the three point bending test of the notched beam, and the flexural properties by the four point bending test of the rectangular beam. On the other hand, the phenomenon that the flexural strength decreases to the tensile strength with the increase in the concrete beam's depth has been known experimentally [3]. Therefore, the two dimensional nonlinear FEM analysis was conducted for rectangular beams by using mechanical characteristics of PFC in order to investigate the size dependence of the flexural strength of PFC beams.

2. MECHANICAL TEST FOR PORE FREE CONCRETE

2.1 Test specimens

Materials and mix proportion of PFC are presented in Tables 1 and 2. The constitution of binding materials (B) of PFC was decided by Furnas's closest packing theory (Furnas 1931)

Table 1: Materials

Name		Property
Binding materials (B)	Low-heat-Portland Cement (LC)	Specific surface area: 3330 cm ² /g, Density: 3.24 g/cm ³
	Powder of quartz (Q)	Density: 2.59 g/cm ³
	Silica fume (SF)	Specific surface area: 20 m ² /g, Density: 2.29 g/cm ³
Sand	Silica sand (S)	Max size: 0.3 mm, Density: 2.61 g/cm ³
Short fiber	Steel fiber (F)	Diameter: 0.2 mm, Density: 7.84 g/cm ³ , length: 15 mm, Tensile strength: 2800 MPa
Admixture	Superplasticizer (SP)	Polycarboxylic acid-based
	Deforming agent (DF)	Polyglycolic acid-based

Table 2: Mix proportion

Name	Unit weight (kg/m ³)							
	W	B			S	F	SP*	DF*
		C	Q	SF				
PFC-0	199	876	347	102	927	0 (0 vol.%)	B × 2.8%	B × 0.02%
PFC-2						157 (2 vol.%)		

* Admixture: Inner split replacement for water

so that the binding materials formed the maximum density grading. In this study, the mixing volume ratio of each binding material of PFC is LC : Q : SF=6 : 3 : 1. Steel fibers were mixed into the specimens, and the mixing volume of the fiber was 2 vol. %. PFC was mixed using 30 L mixers. After casting, the sealed curing was conducted for 48 hours. After the form removal, the deaerating process was also carried out for 30 minutes to absorb the water into specimens. In this process, the specimens were completely immersed in water within a closed vessel, then the air was removed from the specimens and also the water was supplied to the interior of them by reducing the pressure inside of the vessel. When the water-absorbing process was finished, the specimens were cured with steam (90 °C) for 48 hours, and then a heat curing process (1 atm, 180 °C) for 48 hours was carried out.

2.2 Method of mechanical test

Figure 1(a) shows the size of the specimen for compression test and splitting cylinder test. The compression test was conducted in accordance with the test method in JIS A 1108 “Method of test for compressive strength of concrete” in order to investigate the compressive strength f_c' of PFC. In the compression test, longitudinal strain and transverse strain were measured by using 30 mm long strain gauges, and the static modulus of elasticity E_c and Poisson’s ratio were calculated. In the splitting cylinder test, 30 mm long strain gauges were attached on the surfaces of one end in the specimen, perpendicular to the direction of the force in order to continually observe the load and strain relationship. This method was introduced in the guidelines of Japan Society of Civil Engineers “Recommendations for design and construction of ultra-high strength fiber reinforced concrete structures (Draft) [4]” (hereafter, JSCE guidelines), where the strain value can identify exactly the moment of the first crack’s occurrence by tracking the discontinuity. The stress when the first crack occurred is defined as a cracking strength f_{cr} in the splitting cylinder test.

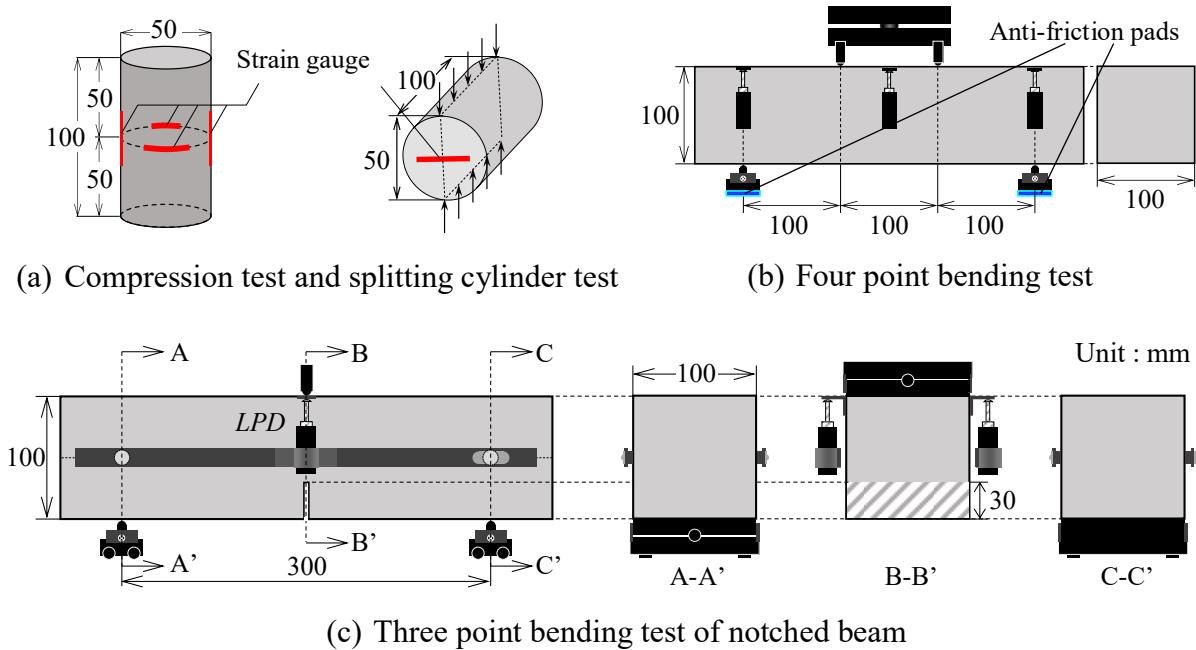


Figure 1: Measurements and size of the specimens

Four point bending tests were carried out using a rectangular beam with the geometry of $100 \times 100 \times 400$ mm as shown in Figure 1(b). Three displacement transducers were installed to measure the deflection of beams during the loading test. Furthermore, anti-friction pads using Teflon sheets and silicon grease were inserted between supports and loading machine in order to prevent the horizontal friction. In this study, the tests were continued until the deflection reached 10 mm.

Three point bending tests were also conducted based on JCI-S-002-2003 which was stipulated by Japan Concrete Institute (JCI) [5]. The specimen's dimension was $100 \times 100 \times 400$ mm as shown in Figure 1(c). All specimens were notched by a concrete saw at the mid-span after the all curing processes, and then three point bending tests of these beams were conducted. Displacement transducers were installed to measure the loading point displacement (*LPD*) of the both sides of the beams during the loading test based on JCI-S-002-2003. In this study, these tests were continued until *LPD* reached 15 mm. In addition, the tension softening curves were estimated by using the program proposed by Japan Concrete Institute. The tension softening curve was estimated by the inverse analysis and the poly-linear approximation using the data of the Load-*LPD* curves of a notched beam. Finally, the area below the estimated tension softening curve was determined as the fracture energy.

2.3 Experimental results and discussion

The characteristic values of PFC obtained from the compression test, splitting cylinder test and four point bending test were shown in Table 3. The compressive strength f_c' of non-fiber reinforced specimen of PFC (PFC-0) was 411 MPa, while that of PFC-2 was 330 MPa. It indicates the compressive strength of PFC-2 was decreased by 20% compared with that of PFC-0 due to the using of short steel fibers. Moreover, the elastic modulus E_c of PFC was

Table 3 : Characteristic values of PFC obtained from the each strength tests

Name	Fiber Volume (vol.%)	Compressive strength (MPa)	Cracking strength (MPa)	Flexural Strength (MPa)	Elastic modulus (GPa)	Poisson's ratio
PFC-0	0.0	411	—	—	—	—
PFC-2	2.0	330	12.2	23.3	60.7	0.184

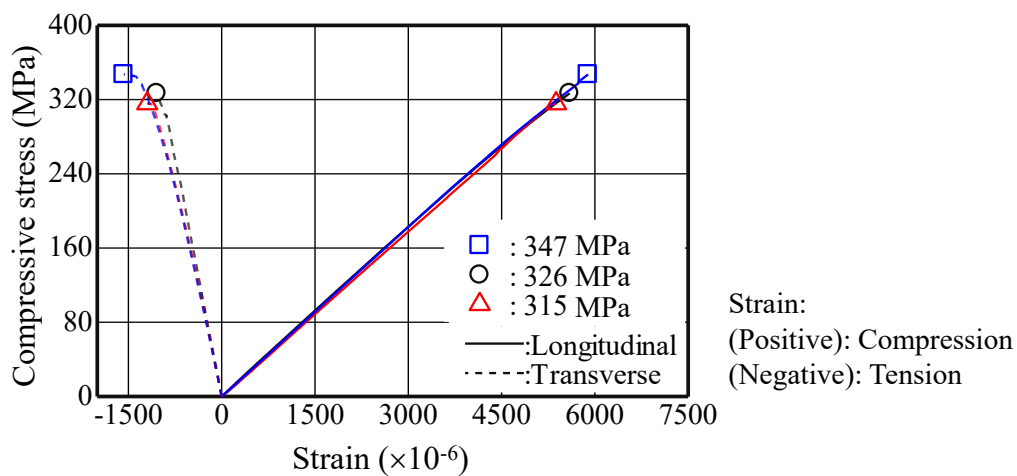


Figure 2 : Compressive stress – strain relationships of PFC-2

larger than 60 GPa with Poisson's ratio about 0.18, which showed similar values with normal strength concrete. Figure 2 shows the relationships between compressive stress and strain. The stress-longitudinal strain curves of PFC showed the linear-elastic behaviour up to the ultimate strength, and the strain at the peak stress was more than 5000×10^{-6} . The failure behaviour of all specimens for the compression test was very brittle and some of the specimens were divided into several pieces after the peak load in spite of the reinforcement by short steel fibers. In general, the volume content of the entrapped air is increased by adding fibers. In the case of PFC-2, it was assumed that the entrapped air affected on the decrement of the compressive strength of PFC.

The cracking strength f_{cr} of PFC-2 was 12.2 MPa, and this value was very low compared with the compressive strength of PFC-2. The relationships between flexural stress and deflection, and the flexural crack pattern at the constant moment region in four point bending test of rectangular beams are shown in Figures 3 and 4, respectively. The average flexural cracking strength when the initial crack occurred was 13.5 MPa, then the flexural stress increased until the average flexural strength of 23.3 MPa. Furthermore, just before the flexural strength, the cracks were well distributed at the bottom of the constant moment region and the average crack spacing was only 3 to 4 mm. On the other hands, the deformation of the beams was concentrated on a single flexural crack after the flexural strength developed, then the flexural stress gradually decreased as the crack opening increased. Generally, the flexural stress in the bending test will be suddenly decreased just after the cracking in the case of non-reinforced cementitious material. Therefore, it was confirmed that the steel fiber

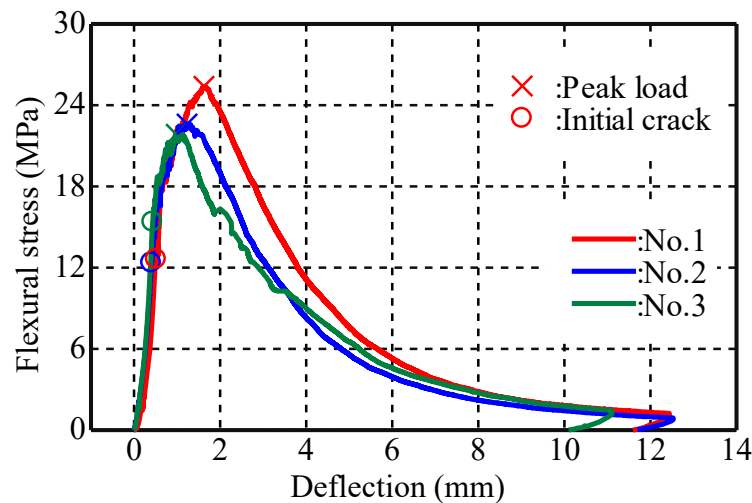
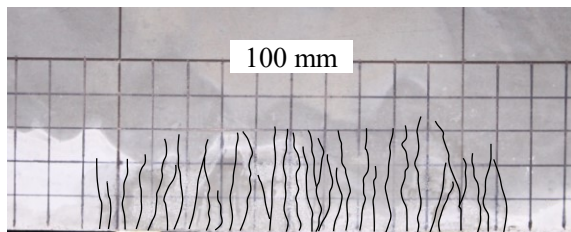


Figure 3 : Flexural stress – deflection curves in the 4 point bending tests



(a) Just before the flexural strength



(b) After the flexural strength

Figure 4 : Crack distribution at the beam's constant moment region (Specimen No.1)

Table 4 : Characteristic values of bending test and tension softening curve

Name	Average peak load (kN)	G_F (N/mm)	f_t (MPa)	Crack width, w_1 (mm)	Crack width, w_2 (mm)
PFC-2	25.7	18.3	7.84	0.53	4.55

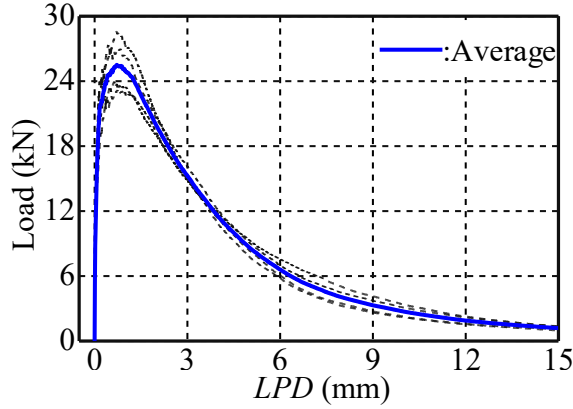


Figure 5 : Load – LPD curves

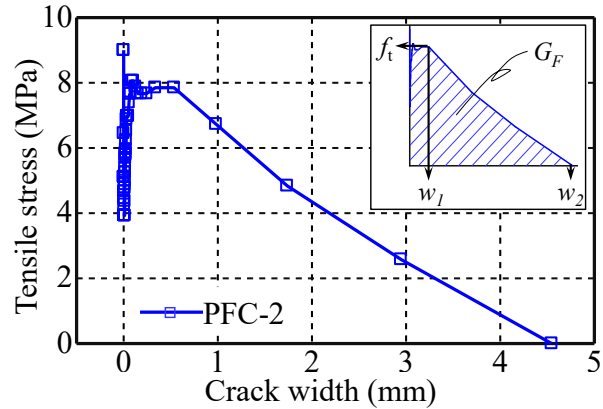


Figure 6 : Tension softening curve

reinforcement can improve the crack distribution and the flexural strength of PFC.

The characteristic values obtained from the three point bending tests of notched beams and tension softening curves are shown in Table 4. Figure 5 shows the Load-LPD curves of PFC-2. In this figure, the dotted lines show the results of each specimen and the solid line shows the average of four specimens. In this test, the concrete crushing under the loading point were not observed. The tension softening curve estimated from poly-linear approximation using the averaged data of the Load-LPD curves of PFC notched beams, is shown in Figure 6. In this study, the second peak stress in the tension softening curve was defined as a tensile strength f_t . The tensile strength f_t and the crack width w_1 at the end of the plateau of tension softening curve are shown in Table 4. In addition, the values of the crack width w_2 where the stress comes to 0 were estimated from the last two points of the tension softening curve by extending the straight line to zero-stress level based on the linear interpolation of the last two point. In this tension softening curve, there were three parts: 1. the part where the tensile stress decreased immediately just after the cracking, 2. the part where the stress increased again due to the influence of the bridging effect of steel fibers, 3. the part where the stress gradually dropped to zero as the crack opening increased. From the above reasons, the flexural ductility of the beams of PFC can be improved by the mixing of steel fibers.

3. FINITE ELEMENT ANALYSIS OF RECTANGULAR BEAM

3.1 Analytical method

The phenomenon that the flexural strength decreases to the tensile strength with the increase in the concrete beam's height has been known experimentally. In this study, the two dimensional nonlinear FEM analysis using DIANA system (version 9.6) was conducted for rectangular beams in order to investigate the size dependence of the flexural strength of PFC beams. In this analysis, a finite element model of interface element at the mid span was defined based on the discrete cracking model and the nonlinear material parameters were specified for discrete cracking in the interface: the tensile strength, the tension softening curve

from experimental results. Furthermore, the concrete element was defined as a linear elastic model so the elastic modulus and Poisson's ratio were determined from experimental results. Displacement control with Modified Newton-Raphson method was adopted to solve equilibrium equations. When the variation of internal energy has become less than 0.01% of the internal energy of the first iteration in the step, the iteration process was terminated to move to the next step.

3.2 Analytical cases

Table 5 shows all analytical cases and input values for E_c , Poisson's ratio, the each mesh size and the beam's height in the 4 cases of PFC rectangular beam. The size of all square elements was decided based on the beam's height as shown in Figure 7. To investigate the influence of the beam's height, the beams of all analytical cases have the same width of the web 100 mm. In addition, the same poly-linear tension softening curve based on the experimental result of PFC-2 was input as the interface material characteristics for all analytical cases. The crack was modelled by separating the nodes in this analysis. In this discrete cracking model, the bridging force across the interface element was decided by the tension softening curve of PFC.

3.3 Analytical results and discussion

Table 6 shows the summary of the analytical results for the four point bending test of PFC-2. The flexural stress-deflection curves of each case and the experimental result are shown in Figure 8. The experimental result is the averaged flexural stress-deflection curve from the results of the four point bending test for rectangular beams with the dimension of 100×100×400 mm. In the beam with the dimension of 100×100×400 mm, the peak flexural

Table 5 The values for the factors in this analysis

Dimension (width×height×length)	Height, h (mm)	Mesh size (mm)	E_c (GPa)	Poisson's ratio
100×100×400	100	2	60.7	0.18
100×150×600	150	3		
100×200×800	200	4		
100×400×1600	400	8		

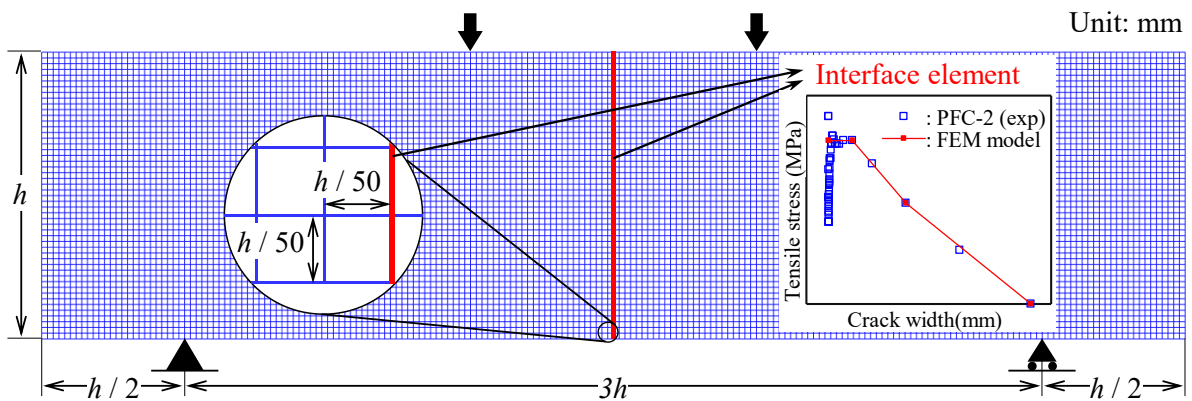


Figure 7: 2D FEM model and tension softening model for rectangular beam

Table 6 : Summary of the results of FEM analysis

Dimension (width×height×length)	Height, h (mm)	Tensile strength, f_t (MPa)	Flexural strength, f_b (MPa)	f_b / f_t
100×100×400(EXP)	100	7.84	23.3	2.97
100×100×400(FEM)	100		21.8	2.78
100×150×600	150		21.3	2.72
100×200×800	200		20.8	2.65
100×400×1600	400		19.5	2.49

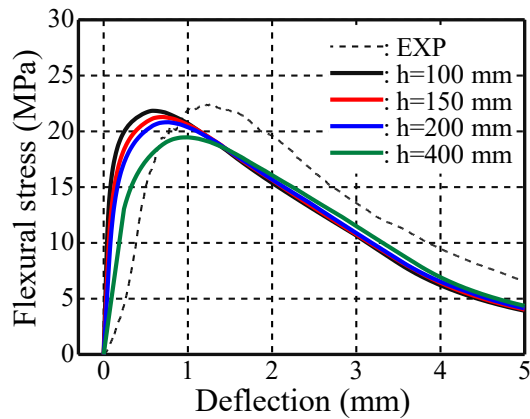


Figure 8 : Flexural stress—deflection curves in FEM analysis

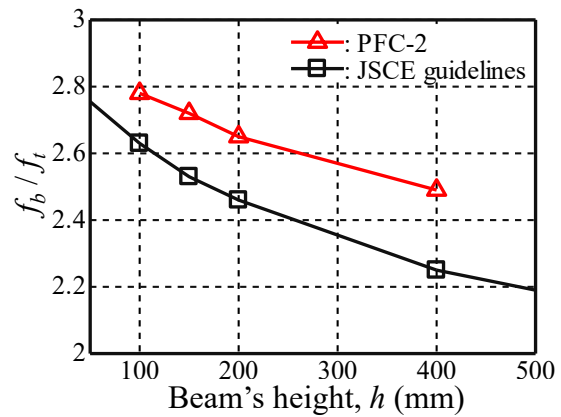


Figure 9 : Size dependence of flexural strength for PFC-2

stress and post peak behaviour of the analytical result were very similar to those of experimental results. However, the pre peak stiffness of analytical result was quite high compared with the experimental result. In this analysis, the deformation of the beam was concentrated on an interface element while the beam's cracks were distributed at the constant moment region in the experiment.

Figure 9 shows the relationships between the beam's height and the ratio of flexural strength f_b to f_t of PFC-2. The flexural strength of the analytical beams gradually decreased with the increase in the beam's height. The relationship of the ultra-high strength fiber reinforced concrete proposed by JSCE guidelines were also shown in this figure. These results indicate that PFC-2 have almost same size dependence of flexural strength compared with the ultra-high strength fiber reinforced concrete (UFC).

4. CONCLUSIONS

- The compressive strength and elastic modulus of Pore Free Concrete (PFC) with short steel fibers was larger than 300 MPa and 50 GPa, respectively.
- The relationships between compressive stress and longitudinal strain in the compression test were almost linear until the peak load.
- The flexural strength and flexural ductility of PFC rectangular beams can be improved by using short steel fibers.
- In the Finite Element Analysis of PFC rectangular beams, the flexural strength became smaller with the increase in the beam's height.

REFERENCES

- [1] Kono, K., Nakayama, R. and Tada, K. (2015) “Development of the World’s Highest Strength Cementitious Material”, *Journal of Research of the Taiheiyo Cement Corporation*, 169: 20-29.
- [2] C. C. Furnas. (1931) “Grading aggregate I – Mathematical relations for beds of broken solids of maximum density”, *Industrial and Engineering Chemistry*, 23(9): 1052-1058
- [3] Uchida, Y., Rokugo, K., Koyanagi, W. (1992) “Application of Fracture Mechanics to Size Effect on Flexural Strength of Concrete”, *Proceedings of JSCE, Concrete Engineering and Pavements*, No.442, pp. 101-107.
- [4] Japan Society of Civil Engineers (JSCE), “Recommendations for Design and Construction of Ultra High Strength Fiber Reinforced Concrete Structures (Draft)”, *Concrete Library No.113* (2004, in Japanese).
- [5] Japan Concrete Institute. (2003) “JCI-S-002-2003: Method of test for load-displacement curve of fiber reinforced concrete by use of notched beam”, Japan Concrete Institute Standard, http://www.jci-net.or.jp/j/jci/study/jci_standard/JCI-S-002-2003-e.pdf.

